Linearized Theory of Finite Cavity Flow around a Thin Jet-Flapped Hydrofoil

Teruhiko Kida* and Yoshihiro Miyai†
University of Osaka Prefecture, Sakai, Osaka, Japan

A theoretical analysis of the steady finite cavity flow around a thin plane hydrofoil with a thin jet flap is presented. Distributions of sources and vorticies are used to obtain a governing equation of this cavity flow. The resulting equation is solved by the method of matched asymptotic expansions for small value of the jet-momentum coefficient. Using the present method, there are three cavity models around conventional hydrofoils: open model; closed; and semiclosed models. It is found that the open cavity model is reasonable from a theoretical viewpoint and other cavity models are unreasonable.

Introduction

IT is well known that the principle of the jet flap is to create jet-induced pressure lift by means of a high-momentum jet sheet. There are numerous research papers, dealing with theoretical and experimental aspects of fully wetted, jet-flapped wings.[1] On jet-flapped supercavitating foils, many theoretical[2-5] and a few experimental[6] studies have been published. In particular, Ho[2] solved the problem of an inviscid, incompressible, uniform flow passing over a thin jet-flapped, supercavitating foil, by considering the "zero-thickness" jet as vortex sheet which is suggested by Spence.[7] Since Ho's work was reported, many theoretical studies have been reported on this problem, and it has become clear that the Spence's model of a jet flap on a wetted aerofoil is applicable to a supercavitating jet-flapped foil. These theoretical analyses treated only jet-flapped supercavitating foils with infinite cavities, and we have not found to date theoretical work on a jet-flapped supercavitating hydrofoil with a finite cavity. However, conventional supercavitating hydrofoils with finite cavities have been studied theoretically and many flow models have been proposed, in order to decide on the flow model for cavity closure and the wake behind the closure which gives the best representation of the very complicated real flow. There are many well-known nonlinear models of supercavitating flows with a finite cavity; Riabouchinsky's model, re-entrant jet model, Rosko's model, Wu's model and Tulin's single and double spiral vortex model.[8] Theoretical analyses with these nonlinear flow models are complicated and also present difficulties in obtaining expressions for the foil performance characteristics. Because of the abovementioned difficulties, linearized flow models, such as the closed, semiclosed and open models, the linearized Rosko model, the linearized double-spiral vortex model and generalized Riabouchinsky model, have been used.[9]

One of the purposes of this paper is to decide which linearized flow model should be applied to a jet-flapped supercavitating hydrofoil with a finite cavity without involving theoretical contradication. In this paper, the three models (closed, semiclosed, and open) which can be represented by means of the Tulin's source-sink method are considered and only the open model is cleared to be reasonable and provable theoretically for a jet-flapped supercavitating hydrofoil with a finite cavity.

Received September 9, 1974; revision received November 14, 1974.
Index categories: Hydrodynamics; Jets, Wakes, and Viscid-Inviscid Flow Interactions.

*Associate Professor of Mechanical Engineering.
†Professor of Mechanical Engineering.

Theoretical Analysis

Derivation of Basic Equations

Consider an inviscid, incompressible, uniform flow of velocity U_0 passing over a thin hydrofoil at an incidence α, at the trailing edge of which a thin jet sheet issues at deflection angle τ with respect to the chord line. Both α and τ are considered to be small such that the linearized theory may be applied. It is convenient to refer all lengths to the chord length, speeds to the uniform flow velocity and pressures to ρU_0^2. The cavity length is taken as ℓ, and the ordinates of the jet sheet and the upper boundary of the cavity are taken as $y_j(x)$ and $y_c(x)$, respectively, as shown in Fig. 1. Let C_j be the jet-momentum coefficient. Then, according to Spence,[7] the "zero-thickness" jet can be considered as $\Delta p=(C_j/2)\,(d^2y_j/dx^2)$ where Δp is the pressure difference between the upper and lower boundaries of the jet sheet. As the lower boundary of the cavity is just the upper boundary of the jet sheet, the linearized conditions along the real axis in the physical plane are specified as follows:

1) On the foil,

$$u=\sigma/2+f(x), \qquad v=-\alpha \qquad \text{for } 0<x<1$$

2) On the cavity,

$$u=\sigma/2, \qquad v=y_c'(x) \qquad \text{for } 0<x<\ell$$

$$u=u_a(x)+C_j y_j''(x)/4, \qquad v=y_j'(x) \qquad \text{for } \ell<x$$

3) On the jet sheet,

$$u=\sigma/2-C_j y_j''(x)/2, \qquad v=y_j'(x) \qquad \text{for } 1<x<\ell$$

$$u=u_a(x)-C_j y_j''(x)/4, \qquad v=y_j'(x) \qquad \text{for } \ell<x$$

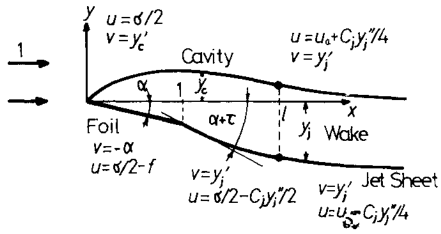

Fig. 1 Sketch showing a jet-flapped supercavitating hydrofoil with a finite cavity and the linearized boundary conditions.

Here, f is like a vortex density distribution and u_a is mean velocity between the upper and lower edges of the wake; u and v denote the disturbed velocities along the x and y-axis. For convenience, we take the leading edge as the origin, and the x-axis in the direction of undisturbed flow, the y-axis upwards; σ is the cavitation number.

The strengths of the elemental source and vortex distribution along the x-axis are taken as $m(x)$ and $\gamma(x)$, respectively. Applying the relation

$$\lim_{y\to\pm 0}\int_0^c yf(\xi)d\xi/[(x-\xi)^2+y^2]=\pm\pi f(x)$$

and using the previous boundary conditions,

$$\begin{aligned} m(x)&=\alpha+y_c'(x), & \gamma(x)&=-f(x) & &\text{for } 0<x<1\\ &=y_c'(x)-g_c(x), & &=(C_j/2)g_c'(x) & &\text{for } 1<x<\ell\\ &=0, & &=(C_j/2)g_0'(x) & &\text{for } \ell<x \end{aligned} \tag{1}$$

Using

$$\lim_{y\to\pm 0}\int_0^c (x-\xi)f(\xi)d\xi/[(x-\xi)^2+y^2]=\int_0^c f(\xi)d\xi/(x-\xi)$$

$$\begin{aligned} 1/\pi\int_0^\ell m(\xi)d\xi/(x-\xi)&=\sigma+f(x) & &\text{for } 0<x<1\\ 1/\pi\int_0^\ell m(\xi)d\xi/(x-\xi)&=\sigma-(C_j/2)g_c'(x) & &\text{for } 1<x<\ell\\ 1/\pi\int_0^\ell m(\xi)d\xi/(x-\xi)&=u_a-(C_j/2)g_0'(x) & &\text{for } \ell<x \end{aligned} \tag{2}$$

and

$$\begin{aligned} 1/\pi\int_0^\infty \gamma(\xi)d\xi/(x-\xi)&=2\alpha-m(x) & &\text{for } 0<x<1\\ 1/\pi\int_0^\infty \gamma(\xi)d\xi/(x-\xi)&=-2g_c(x)-m(x) & &\text{for } 1<x<\ell\\ 1/\pi\int_0^\infty \gamma(\xi)/(x-\xi)&=-2g_0(x) & &\text{for } \ell<x \end{aligned} \tag{3}$$

where $g_c\equiv y_j'(x)$ for $1<x<\ell$, $g_0\equiv y_j'(x)$ for $\ell<x<\infty$. From Eq. (2), m for $0<x<\ell$ is derived by using the Carlemann-Betz inverse formula.

$$m(x)=\frac{H(x)}{\pi}\left[\int_0^1\frac{f(\xi)d\xi}{H(\xi)(\xi-x)}-\frac{C_j}{2}\times\int_1^\ell\frac{g_c'(\xi)d\xi}{H(\xi)(\xi-x)}\right]+\sigma H(x)+C\frac{H(x)}{\ell-x} \tag{4}$$

where $H(x)=(\ell/x-1)^{1/2}$ and C is the integral constant. Here, the new variables X and Y are defined as $X^2=\ell x/(\ell-x)$ for $0<x<\ell$, $Y^2=\ell x/(x-\ell)$ for $x>\ell$, and $f(X)$, $g_c(X)$, $g_0(Y)$ are also defined as $f(X)=f(x)$, $g_c(X)=g_c(x)$, $g_0(Y)=g_0(x)$, respectively. Then, when Eq. (4) is substituted into the first line of Eq. (3) and the new variables are used, the function $f(X)$ is derived, by means of the Carlemann-Betz inverse formula.

$$\begin{aligned} f(X)=\frac{\ell+X^2}{2XI(X)}\Bigg[&\frac{K}{a-X}-C_0-\frac{2\alpha}{\pi}\int_0^a\frac{\nu I(\nu)}{\ell+\nu^2}\frac{d\nu}{\nu-X}\\ &+\frac{\sigma\ell^{1/2}}{\pi}\int_0^a\frac{I(\nu)}{\ell+\nu^2}\frac{d\nu}{\nu-X}+\frac{C_j}{2\pi^2}\\ &\times\int_0^a\frac{I(\nu)d\nu}{\nu-X}\int_{\ell^{1/2}}^\infty\frac{\nu}{\mu^2+\nu^2}\times\frac{\mu^2-\ell}{\ell^2}g_0'(\mu)d\mu\\ &-\frac{C_j}{2\pi}\int_a^\infty\frac{\ell+\nu^2}{\ell^2}\frac{I(\nu)}{\nu-X}g_c'(\nu)d\nu\Bigg]\quad\text{for } 0<X<a \end{aligned} \tag{5}$$

where $g_0'(X)$ and $g_c'(X)$ are the differential with respect to X, K the integral constant and $C_0=C/\ell^{3/2}$ and $I(X)=(X/|a-X|)^{1/2}$. Substituting Eqs. (4) and (5) into the second line of Eq. (3), the relation between the function g_c and g_0 is derived as

$$\begin{aligned} g_c(X)\frac{2X}{\ell+X^2}=\frac{1}{I(X)}\Bigg[&\frac{C_j}{2\pi}\int_a^\infty\frac{\ell+\nu^2}{\ell^2}\frac{I(\nu)}{\nu-X}g_c'(\nu)d\nu\\ &-\frac{C_j}{2\pi}\int_{\ell^{1/2}}^\infty\frac{X}{X^2+\mu^2}\frac{\mu^2-\ell}{\ell^2}g_0'(\mu)d\mu\\ &-\frac{C_j}{2\pi^2}\int_{\ell^{1/2}}^\infty\frac{g_0'(\mu)}{X^2+\mu^2}\frac{\mu^2-\ell}{\ell^2}d\mu\\ &\times\int_0^a I(\nu)\frac{\mu^2-X\nu}{\nu^2+\mu^2}d\nu+\frac{2\alpha}{\pi}\int_0^a\frac{\nu I(\nu)}{\ell+\nu^2}\frac{d\nu}{\nu-X}\\ &-\frac{\sigma\ell^{1/2}}{\pi}\int_0^a\frac{I(\nu)}{\ell+\nu^2}\frac{d\nu}{\nu-X}\Bigg]\\ &-\frac{\sigma\ell^{1/2}}{\ell+X^2}+K\frac{I(X)}{X}+\frac{C_0}{I(X)} \end{aligned} \tag{6}$$

Now, let us evaluate the integral constant K. As the jet sheet issues at the deflection angle τ with respect to the chord line, the boundary condition of $g_c(X)$ at $X=a$ is given as

$$g_c(a)=-(\alpha+\tau) \tag{7}$$

In Eq. (6), when we take the limit of $X\to a$ and consider the above condition (7), it is easily seen that

$$K=0 \tag{8}$$

Substituting Eqs. (5), (6), and (8) into the last line of Eq. (3),

$$\begin{aligned} \frac{2g_0(Y)}{Y^2-\ell}=&-\frac{2\alpha}{\pi}\int_0^a\frac{\nu I(\nu)}{\ell+\nu^2}\frac{d\nu}{\nu^2+Y^2}\\ &+\frac{\sigma\ell^{1/2}}{\pi}\int_0^a\frac{I(\nu)}{\ell+\nu^2}\frac{d\nu}{\nu^2+Y^2}\\ &-\frac{C_j}{2\pi}\int_a^\infty\frac{\ell+\nu^2}{\ell^2}\frac{I(\nu)}{\nu^2+Y^2}g_c'(\nu)d\nu\\ &-\frac{2\alpha}{\pi^2}\int_0^a\frac{\nu I(\nu)}{\ell+\nu^2}\frac{d\nu}{\nu^2+Y^2}\int_0^a\frac{(\mu+\nu)d\mu}{I(\mu)(\mu^2+Y^2)}\\ &+\frac{\sigma\ell^{1/2}}{\pi^2}\int_0^a\frac{I(\nu)}{\ell+\nu^2}\frac{d\nu}{\nu^2+Y^2}\int_0^a\frac{(\mu+\nu)d\mu}{I(\mu)(\mu^2+Y^2)}\\ &-\frac{C_j}{2\pi^2}\int_a^\infty\frac{\ell+\nu^2}{\ell^2}\frac{I(\nu)}{\nu^2+Y^2}g_c'(\nu)d\nu\int_0^a\frac{(\mu+\nu)d\mu}{I(\mu)(\mu^2+Y^2)}\\ &+\frac{C_j}{2\pi}\int_{\ell^{1/2}}^\infty\frac{g_0'(\mu)}{\mu^2-Y^2}\frac{\mu^2-\ell}{\ell^2}d\mu+\frac{C_j}{2\pi^2}\int_0^a\frac{\nu I(\nu)}{\nu+Y^2}d\nu\\ &\times\int_{\ell^{1/2}}^\infty\frac{g_0'(\mu)}{\mu^2+\nu^2}\frac{\mu^2-\ell}{\ell^2}d\mu-C_0\int_0^a\frac{d\nu}{I(\nu)(\nu^2+Y^2)}\\ &+\frac{C_j}{2\pi^3}\int_0^a\frac{\nu I(\nu)}{\nu^2+Y^2}d\nu\int_0^a\frac{(\xi+\nu)d\xi}{I(\xi)(\xi^2+Y^2)}\\ &\times\int_{\ell^{1/2}}^\infty\frac{g_0'(\mu)}{\mu^2+\nu^2}\frac{\mu^2-\ell}{\ell^2}d\mu\quad\text{for } Y>\ell^{1/2} \end{aligned} \tag{9}$$

Next, let us consider the integral constant C_0. The function $g_0(Y)$ for $Y\to\infty$ (i.e., at the cavity termination) is given from Eq. (9) as $g_0 \sim \alpha_i + 0(Y^{-2})$ for $Y\to\infty$, where α_i is the constant easily derived from Eq. (11). Meanwhile from Eq. (6), $g_c \sim C_0 X + \alpha_i + 0(X^{-1})$ for $X\to\infty$, the 3rd and 6th terms of the right-hand side of Eq. (9) can not be integrated, if $C_0 \neq 0$. Therefore, at least, the following condition is required, viz,

$$C_0 = 0 \tag{10}$$

For a conventional hydrofoil, this condition, Eq. (10), is in general not needed, as the relation (9) does not arise. Hence, several models for a conventional hydrofoil can be considered, such as an open cavity model, semiclosed model and closed model. But the condition (10) on a jet-flapped hydrofoil means that the open model only exists reasonably within the limits of this potential flow analysis.

Let us consider the relation between the cavitation number σ and the cavity length ℓ. This relation can be derived from the fact that the leading edge singularity is of $0(x^{-1/4})$ in the linearized flows on a supercavitation foil. From this singularity and Eq. (5), the following implict relationship between σ and ℓ is obtained:

$$-\frac{2\alpha}{\pi}\int_0^a \frac{I(\nu)}{\ell+\nu^2}d\nu + \frac{\sigma\ell^{1/2}}{\pi}\int_0^a \frac{I(\nu)d\nu}{\nu(\ell+\nu^2)} - \frac{C_j}{2\pi}\int_a^\infty \frac{I(\nu)}{\nu}\frac{\ell+\nu^2}{\ell^2}g_c'(\nu)d\nu + \frac{C_j}{2\pi^2}\int_0^a I(\nu)d\nu\int_{\ell^{1/2}}^\infty \frac{g_0'(\mu)}{\mu^2+\nu^2}\frac{\mu^2-\ell}{\ell^2}d\mu = 0 \tag{11}$$

Solution $g_c(X)$ for Small C_j

Let us obtain the function $g_c(X)$ from Eq. (6) in the case of the small C_j. The asymptotic expansion method introduced by the previous paper[10] is applied to Eq. (6). The inner solution of g_c near the trailing edge and its outer solution far distance from the trailing edge are easily given by using the previous method.[10] However we will find that the solution by which Eq. (6) is satisfied exactly in the whole region $a<X<\infty$ cannot be obtained by only these inner and outer solutions.

Let define the small perturbation parameter ϵ as $\epsilon \equiv C_j(\ell + a^2)^2/(4a\ell^2)$. The new variable is taken as $\bar{X} = X - a$, and $G_c(\bar{X})$ is defined as

$$G_c(\bar{X}) \equiv (a+\bar{X})^{1/2} g_c(\bar{X})\;[\ell + (a+\bar{X})^2]/\ell^2$$
$$\equiv -a^{1/2}(\ell+a^2)\;[\alpha + \alpha G_\alpha(\bar{X}) + \tau G_\tau(\bar{X})]/\ell^2$$

Moreover, since $\sigma\ell^{1/2} = \alpha\bar{\sigma}_\alpha + \tau\bar{\sigma}_\tau$, the inner solution $G_\alpha^i(\bar{X})$ and the outer solution $G_\alpha^0(\bar{X})$ of $G_\alpha(\bar{X})$ are given by following the previous asymptotic expansion method.[10]

$$G_\alpha^i(\bar{X}) \cong -\frac{B_\alpha}{2}\frac{(\pi\epsilon)^{1/2}}{2i}\times\int_{c-i\infty}^{c+i\infty}(\bar{X}/\epsilon)^{1-s}\frac{F_0(s)}{s-1}ds,\; 0<c<1/2$$

$$G_\alpha^0(\bar{X}) \cong -1 - \frac{\ell+(a+\bar{X})^2}{a^{1/2}(\ell+a^2)}\Bigg[\bar{X}^{1/2} - (a+\bar{X})^{1/2} + \frac{\bar{X}^{1/2}}{a+\bar{X}}\times\frac{1}{\pi}\int_0^a I(\nu)\frac{\ell-\nu(a+\bar{X})}{\ell+\nu^2}d\nu - \frac{\bar{\sigma}_\alpha}{2}\frac{\bar{X}^{1/2}}{a+\bar{X}} + \frac{\bar{\sigma}_\alpha\bar{X}^{1/2}}{a+\bar{X}}\frac{1}{2\pi}\int_0^a I(\nu)\frac{\nu+a+\bar{X}}{\ell+\nu^2}d\nu\Bigg]$$

$$G_\alpha^{0i}(\bar{X}) \cong B_\alpha \bar{X}^{1/2} \tag{12}$$

where

$$B_\alpha \cong -\frac{1}{a^{1/2}} - \frac{a^{-3/2}}{\pi}\int_0^a I(\nu)\frac{\ell-a\nu}{\ell+\nu^2}d\nu + \frac{\bar{\sigma}_\alpha}{2}a^{-3/2} - \frac{\bar{\sigma}_\alpha}{2}\frac{a^{-3/2}}{\pi}\int_0^a I(\nu)\frac{\nu+a}{\ell+\nu^2}d\nu$$

and $F_0(s) = \Gamma(s)G_0(s)$, G_0 is the Lighthill function. When $\bar{G}_\tau(\bar{X})$ is defined by

$$\bar{G}_\tau(\bar{X}) \equiv G_\tau(\bar{X}) - \frac{1}{2\pi i}\int_{c-i\infty}^{c+i\infty}(\bar{X}/\epsilon)^{-s}F_0(s)ds$$

the inner solution G_τ^i and the outer solution G_τ^0 of $\bar{G}_\tau(\bar{X})$ are given

$$\bar{G}_\tau^i(\bar{X}) \cong \epsilon\left[\frac{4a}{\ell+a^2} - \frac{1}{a}\right]\frac{1}{2\pi i}\times\int_{c-i\infty}^{c+i\infty}\left[\frac{\bar{X}}{\epsilon}\right]^{1-s}\frac{P(s)}{s-1}F_0(s)ds$$

$$\bar{G}_\tau^0(\bar{X}) \cong \frac{\ell+(a+\bar{X})^2}{2(\ell+a^2)}\Bigg[\frac{\bar{\sigma}_\tau}{\{a(a+\bar{X})\}^{1/2}} + \frac{\bar{\sigma}_\tau}{a+\bar{X}}\left\{\left[\frac{\bar{X}}{a}\right]^{1/2} - \left[\frac{\bar{X}+a}{a}\right]^{1/2}\right\} - \frac{\bar{\sigma}_\tau}{\pi(a+\bar{X})}\left[\frac{\bar{X}}{a}\right]^{1/2}\int_0^a I(\nu)\frac{\nu+a+\bar{X}}{\ell+\nu^2}d\nu\Bigg] + \left[\frac{\epsilon}{\pi\bar{X}}\right]^{1/2}\left[-1 + \frac{a}{a+\bar{X}}\left\{\frac{\ell+(a+\bar{X})^2}{\ell+a^2}\right\}^2\right]$$

$$\bar{G}_\tau^{0i}(\bar{X}) \cong \left[\frac{\epsilon}{\pi}\right]^{1/2}\left[\frac{4a}{\ell+a^2} - \frac{1}{a}\right]\bar{X}^{1/2} + B_\tau\bar{X}^{1/2} \tag{13}$$

where

$$B_\tau = \frac{\bar{\sigma}_\tau}{2a^{3/2}}\left[1 - \frac{1}{\pi}\int_0^a I(\nu)\frac{\nu+a}{\ell+\nu^2}d\nu\right]$$

$$P(s) = \frac{s^2}{2} - \left[\frac{1}{2}\frac{\ell+5a^2}{3a^2-\ell}\right]s + c_0$$

$$P(1/2) = -1/2 - \pi^{1/2}B_\tau(\ell+a^2)/[2\epsilon^{1/2}(3a^2-\ell)]$$

and c_0 is constant.

Now, let us consider the asymptotic limit of g_c for $X\to\infty$. From Eqs. (12) and (13), this limit is expressed as $g_c(X) \approx \alpha_i + \ell^2 A_0/X + 0(X^{-2})$, where A_0 is the constant. Since the value of A_0 is not zero, we cannot integrate the 6th term of the right hand side of Eq. (9) yet, since the integrand of this term is of $0(1/\nu)$ for $\nu\to\infty$. Hence, we must consider the asymptotic solution near the cavity termination. The new variable is defined by $T = 1/(X-a)$ and we define the function $G_c(T)$ as $G_c \equiv (aT+1)^{1/2}\{g_c(X) - \alpha_i\}\{\ell T^2 + (aT+1)^2\}/\ell^2$. When the small perturbation parameter Δ is defined as $\Delta \equiv C_j^{1/2}/(2\ell)$, and the inner variable $\bar{T}$ is taken as $\bar{T} = T/\Delta$, the governing equation of the first approximation can be expressed from Eq. (6).

$$G_{c0}(\bar{T}) = A_0\bar{T} + \frac{1}{\pi}\int_0^\infty \frac{G_{c0}'(\bar{t})}{\bar{t}(\bar{t}-\bar{T})}d\bar{t}\; G_{c0}(0) = 0 \tag{14}$$

where the function G_c is expressed as the form; $G_c(T) = \Delta G_{c0}(\bar{T}) + 0(\Delta^2)$. When the following Mellin transformation

$$G_{c0}(\bar{T}) = \frac{1}{2\pi i}\int_{c-i\infty}^{c+i\infty}\bar{T}^{3/2-s}F(s)ds \tag{15}$$

is substituted into Eq. (14), the difference equation is obtained as

$$F(s+2) = (s-3/2)F(s)\tan(\pi s) \qquad (16)$$

where

$$\frac{1}{2\pi i}\left[\int_{c-i\infty}^{c+i\infty} - \int_{c+2-i\infty}^{c+2+i\infty}\right]\bar{T}^{3/2-s}F(s)ds = A_0\bar{T} \qquad (17)$$

Considering the condition (17), the solution $F(s)$ of Eq. (16) is derived as

$$F(s) = 2^{s/2}\Gamma(s/2-3/4)\,[a_0/Q_0(s-5/2) + a_1/Q_0(s-3/2)] \qquad (18)$$

where

$$a_0 = -\pi^{1/2}2^{-5/4}A_0Q_0(0),\ a_1 = -a_0Q_0(0)/Q_0(-1)$$

$$Q_0(s) = \frac{\psi(-s/2-1/2)\psi(s/2+1/4)}{\psi(s/2)\psi(-s/2-3/4)},\ \psi(s) = \frac{G(1-s)}{G(1+s)}$$

and $G(s)$ is the Alexeivski function (see Appendix). From Eqs. (15) and (18), G_{c0} for $\bar{T}\to\infty$ is given as $G_{c0}\cong A_0\bar{T}+0(\bar{T}^2)$ i.e., $g_c\cong\alpha_i+\ell^2A_0/X$ and G_{c0} for $\bar{T}\to 0$ is given as $G_{c0}\cong 0(\bar{T}^{3/2}) = 0(X^{-3/2})$, i.e., $g_c\cong\alpha_i+0(X^{-3/2})$ for $X\to\infty$. Therefore, the integration of the 6th term of the right hand side of Eq. (9) can be calculated by using the composite solution constructed by three solutions; the inner solution $G^i_{\alpha,\tau}$, the outer solution $G^0_{\alpha,\tau}$ and the terminal solution G_c.

Solution $g_0(Y)$ for Small C_j

Substituting the composite solution of the function $g_c(X)$ into Eq. (9), the solution $g_0(Y)$ is obtained as follows:

$$g_0(Y) \cong \frac{Y^2-\ell}{2}\Bigg[-2\left\{\frac{a\epsilon}{\pi(a^2+Y^2)}\right\}^{1/2}\frac{a\tau}{\pi(\ell+a^2)} \times\int_0^a \frac{1}{I(\nu)(\nu^2+Y^2)}\left(\cos\theta_0+\frac{\nu}{Y}\sin\theta_0\right)d\nu$$
$$-\frac{2\alpha}{\pi^2}\int_0^a\frac{\nu I(\nu)}{\ell+\nu^2}\frac{d\nu}{\nu^2+Y^2}\int_0^a\frac{(\mu+\nu)d\mu}{I(\mu)(\mu^2+Y^2)} - \frac{2\alpha}{\pi}\int_0^a\frac{\nu I(\nu)}{\ell+\nu^2}\frac{d\nu}{\nu^2+Y^2} + \frac{\sigma\ell^{1/2}}{\pi}\int_0^a\frac{I(\nu)}{\ell+\nu^2}$$
$$\times\frac{d\nu}{\nu^2+Y^2} + \frac{\sigma\ell^{1/2}}{\pi^2}\int_0^a\frac{I(\nu)}{\ell+\nu^2}\frac{d\nu}{\nu^2+Y^2} \times\int_0^a\frac{(\mu+\nu)d\mu}{I(\mu)(\mu^2+Y^2)} - 2\tau\left[\frac{\epsilon}{\pi}\right]^{1/2}$$
$$\times\frac{a^{3/2}}{(\ell+a^2)(a^2+Y^2)}\Bigg] + 0(\epsilon) \qquad (19)$$

where $\theta_0 = \tan^{-1}(Y/a)$

Lift Coefficient

The velocity U_c along the cavity boundary is given by $U_c = U_0(1+\sigma)^{1/2}$. Since σ is of $0(\alpha,\tau)$ and

$$\int_0^\infty \gamma(x)dx = -2\pi\lim_{x\to\infty}[xg_0(x)]$$

$$\int_1^\infty \gamma(x)dx = C_j(\alpha,\tau)/2$$

are given from Eqs. (1) and (7), hence, the lift coefficient C_L is determined by the behavior of the function $g_0(x)$ at infinity:

$$C_L \cong -4\pi\lim_{x\to\infty}[xg_0(x)] = -4\pi\lim_{Y\to\ell^{1/2}}\left[\frac{\ell^2}{Y^2-\ell}g_0(Y)\right]$$

Therefore, using Eq. (19),

$$C_L \cong -2\pi\ell^2\Bigg[-\frac{\tau a}{\pi\ell}\left\{\frac{C_j}{\pi(\ell+a^2)}\right\}^{1/2} \times\int_0^a\frac{1}{I(\nu)(\nu^2+\ell)}\left(\cos\theta+\frac{\nu}{\ell^{1/2}}\sin\theta\right)d\nu$$
$$-\frac{2\alpha}{\pi}\int_0^a\frac{\nu I(\nu)}{(\ell+\nu^2)^2}d\nu + \frac{\sigma\ell^{1/2}}{\pi}\int_0^a\frac{I(\nu)d\nu}{(\ell+\nu^2)^2} - \frac{2\alpha}{\pi^2}\int_0^a\frac{\nu I(\nu)}{(\ell+\nu^2)^2}d\nu\int_0^a\frac{(\mu+\nu)d\mu}{I(\mu)(\mu^2+\ell)}$$
$$+\frac{\sigma\ell^{1/2}}{\pi^2}\int_0^a\frac{I(\nu)d\nu}{(\ell+\nu^2)^2}\int_0^a\frac{(\mu+\nu)d\mu}{I(\mu)(\mu^2+\ell)} - \tau\left[\frac{C_j}{\pi}\right]^{1/2}\frac{a}{\ell(\ell+a^2)}\Bigg] + 0(C_j) \qquad (20)$$

where $\theta = \tan^{-1}[\ell^{1/2}/a]$.

Relation Between σ and ℓ

Considering the solution $g_0(Y)$ given by Eq. (19), the 4th term of the left-hand side of Eq. (11) is of $0(C_j)$, and the 3rd term is calculated by using the composite solution of $g_c(X)$. Since

$$\int_a^\infty\frac{I(\nu)}{\nu}\frac{\ell+\nu^2}{\ell^2}g_c'(\nu)d\nu = \tau\frac{\ell+a^2}{\ell^2}\left[\frac{\pi}{a\epsilon}\right]^{1/2} + 0(C_j)$$

Eq. (11) becomes

$$\frac{\sigma\ell^{1/2}}{\pi}\int_0^a\frac{I(\nu)d\nu}{\nu(\ell+\nu^2)} = \frac{2\alpha}{\pi}\int_0^a\frac{I(\nu)}{\ell+\nu^2}d\nu + \frac{\tau}{\ell}\left[\frac{C_j}{\pi}\right]^{1/2} + 0(C_j) \qquad (21)$$

Hence, the relation between σ and ℓ is obtained from Eq. (21) as follows:

$$\bar{\sigma}_\alpha = -2\ell^{1/2}\tan(\theta/2-\pi/4) + 0(C_j)$$

$$\bar{\sigma}_\tau = (C_j/\pi)^{1/2}[(\ell+a^2)/\ell]^{1/4}\sec(\theta/2-\pi/4) + 0(C_j) \qquad (22)$$

where $\sigma\ell^{1/2}\equiv\alpha\bar{\sigma}_\alpha+\tau\bar{\sigma}_\tau$ and $\theta = \tan^{-1}[\ell^{1/2}/a]$.

Cavity Shape

The cavity ordinate $y_c(x)$ is related with the source distribution by Eq. (1): $y_c'(x) = -\alpha+m(x)$, for $0<x<1$ and $y_\phi'(\nu) = \xi_\phi(\nu)+\omega(\nu)$ for $1<\nu<\ell$. Using Eqs. (4, 5, and 10),

$$y_c'(X) = \frac{\sigma\ell^{1/2}}{2X} + \frac{\ell+X^2}{X}\Bigg[-\frac{\alpha}{\pi}\left[\frac{X+a}{X}\right]^{1/2}\int_0^a\frac{\mu I(\mu)}{\ell+\mu^2}\frac{d\mu}{\mu+X} + \frac{\sigma\ell^{1/2}}{2\pi}\left[\frac{X+a}{X}\right]^{1/2}\int_0^a\frac{I(\mu)}{\ell+\mu^2}\frac{d\mu}{\mu+X}$$
$$-\frac{C_j}{4\pi}\int_{\ell^{1/2}}^\infty\frac{X}{X^2+\nu^2}\frac{\nu^2-\ell}{\ell^2}g_0'(\nu)d\nu$$

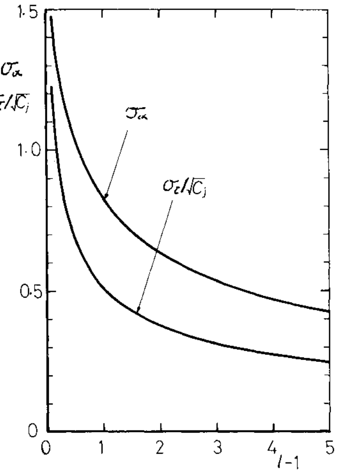

Fig. 2 Relation between the cavitation number and the cavity length in the case of small C_j. σ_α and σ_τ are the derivatives with respect to α and τ.

$$-\frac{C_j}{4\pi}\left[\frac{X+a}{X}\right]^{1/2}\int_a^{\infty}\frac{\ell+\mu^2}{\ell^2}\,\frac{I(\mu)}{\mu+X}\,g_c'(\mu)d\mu$$

$$+\frac{C_j}{4\pi^2}\left[\frac{X+a}{X}\right]^{1/2}\int_0^{a}\frac{I(\mu)}{\mu+X}\,d\mu$$

$$\times\int_{\ell^{1/2}}^{\infty}\frac{\mu}{\nu^2+\mu^2}\,\frac{\nu^2-\ell}{\ell^2}\,g_0'(\nu)d\nu\Big]\quad 0<X<\infty \qquad (23)$$

where $X^2=\ell x/(\ell-x)$. Substituting the solutions $g_0(Y)$ and $g_c(X)$ into Eq. (23) and integrating $y_c'(x)$ with respect to x, the ordinate y_c of the cavity boundary is given as follows:

$$y_{c\alpha}\cong\ell^2\bar{\sigma}_\alpha\int_0^X\frac{dX}{(\ell+X^2)^2}+2\ell^2\int_0^X\frac{\{X(X+a)\}^{1/2}}{(\ell+X^2)^2}$$

$$\times\Big[-\left[\frac{X}{X+a}\right]^{1/2}+\left[\frac{\ell}{\ell+a^2}\right]^{1/4}\Big\{\cos\left[\frac{\theta}{2}-\frac{\pi}{4}\right]$$

$$-\frac{X}{\ell^{1/2}}\sin\left[\frac{\theta}{2}-\frac{\pi}{4}\right]\Big\}\Big]dX$$

$$-\ell^2\bar{\sigma}_\alpha\int_0^X\frac{\{X(X+a)\}^{1/2}}{(\ell+X^2)^2}\Big[\frac{1}{\{X(X+a)\}^{1/2}}$$

$$+\left[\frac{\ell}{\ell+a^2}\right]^{1/4}\Big\{\frac{X}{\ell}\cos\left[\frac{\theta}{2}-\frac{\pi}{4}\right]$$

$$-\frac{1}{\ell^{1/2}}\sin\left[\frac{\theta}{2}-\frac{\pi}{4}\right]\Big\}\Big]dX+0(C_j)$$

$$y_{c\tau}\cong\ell^2\bar{\sigma}_\tau\int_0^X\frac{dX}{(\ell+X^2)^2}-\ell^2\bar{\sigma}_\tau\int_0^X\frac{\{X(X+a)\}^{1/2}}{(\ell+X^2)^2}$$

$$\times\Big[\frac{1}{\{X(X+a)\}^{1/2}}+\left[\frac{\ell}{\ell+a^2}\right]^{1/4}\Big\{\frac{X}{\ell}\cos\left[\frac{\theta}{2}-\frac{\pi}{4}\right]$$

$$-\frac{1}{\ell^{1/2}}\sin\left[\frac{\theta}{2}-\frac{\pi}{4}\right]\Big\}\Big]dX$$

$$+\ell\left[\frac{C_j}{\pi}\right]^{1/2}\int_0^X\left[\frac{X}{X+a}\right]^{1/2}\frac{dX}{\ell+X^2}+0(C_j) \qquad (24)$$

where $y_c(x)=\alpha y_{c\alpha}(x)+\tau y_{c\tau}(x)$.

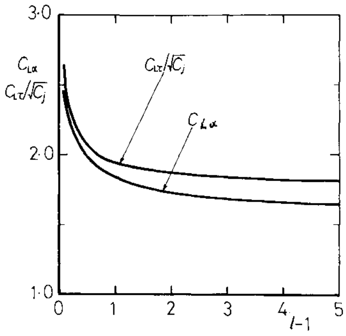

Fig. 3 The lift derivatives $C_{L\alpha}$ and $C_{L\tau}$ against the cavity length in the case of small C_j.

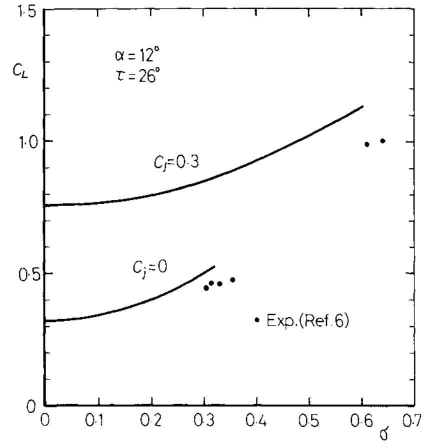

Fig. 4 Comparison of the total lift with the experimental results in the case of $\alpha=9°$ and $\tau=36°$.

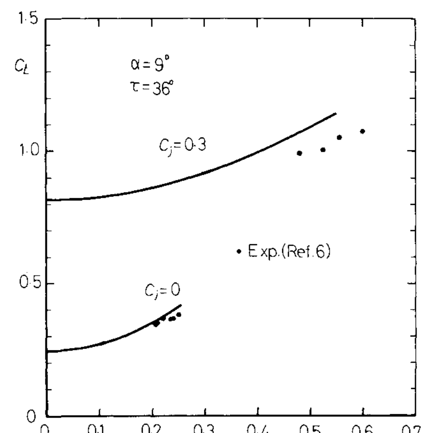

Fig. 5 Comparison of the total lift with the experimental results in the case of $\alpha=12°$ and $\tau=26°$.

Numerical Results

The numerical calculations are carried out by using the Gauss numerical integration (12 points). At first, the relations between $\bar{\sigma}_\alpha$, $\bar{\sigma}_\tau$ and ℓ are obtained by Eq. (22). Since the first approximations of σ_α and $\sigma_\tau/C_j^{1/2}$, compared to C_j, are independent of C_j, respectively, σ_α and $\sigma_\tau/C_j^{1/2}$ are shown in Fig. 2 against the cavity length ℓ. Using these relations, the lift slopes $C_{L\alpha}$ and $C_{L\tau}$ with respect to the incidence and the jet deflection are computed from Eq. (20). Since $C_{L\alpha}$ and $C_{L\tau}/C_j^{1/2}$ are independent of C_j for the first approximation of C_j, $C_{L\alpha}$ and $C_{L\tau}/C_j^{1/2}$ are shown in Fig. 3 against the cavity length. The total lift coefficient C_L for $\alpha=9°$ and $\tau=36°$ is shown in Fig. 4 and for $\alpha=12°$ and $\tau=26°$ in Fig. 5. In these

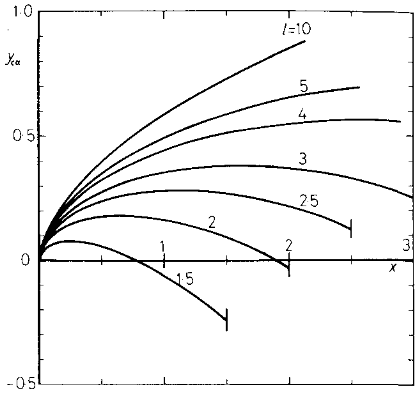

Fig. 6 Cavity shape derivative $y_{c\alpha}$ for the various cavity length in the case of small C_j.

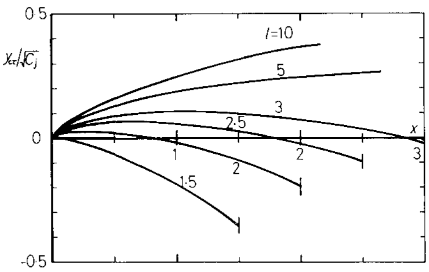

Fig. 7 Cavity shape derivative $y_{c\tau}$ for the various cavity length in the case of small C_j.

figures, the dots (•) are the experimental results by Dinh.[6] The discrepancy between the present results and the experimental results may be caused by the facts that the values of σ, α, τ, and $C_j^{1/2}$ are assumed to be very small and for their squares to be negligibly small. Figures 6 and 7 are the cavity shape derivatives with respect to α and τ. These shapes are calculated by Eq. (24). It is seen from these figures that the cavity thickness near the leading edge can be increased and the foil profile is made to be thicker near the leading edge, by a jet flap.

Therefore, for $s=c+i\eta$, $\eta\to\infty$

$$Q_0(s) \simeq 0(1)$$

Since

$$G(s+1)=(2\pi)^{s/2}\exp\left\{-\frac{s(s+1)}{2}-\frac{\gamma s^2}{2}\right\}$$

$$\times\prod_{n=1}^{\infty}\left\{\left[1+\frac{s}{n}\right]^n\exp\left[-s+\frac{s^2}{2n}\right]\right\}$$

hence

$$Q_0(s)=(2\pi)^{-1/2}\prod_{n=1}^{\infty}\left[\frac{\{1+s/(2n+1)\}\{1-s/(2n-1/2)\}\{1+s/(2n)\}\{1-s/(2n-3/2)\}}{\{1-s/(2n-1)\}\{1+s/(2n+1/2)\}\{1-s/2n)\}\{1+s/(2n+3/2)\}}\right]^n$$

Therefore, it is clear that $Q_0(s)$ has poles of order n at $S=2n$, $2n-1$, $-(2n+1/2)$, $-(2n+3/2)$, zeros of order n at $s=2n-1/2$, $2n-3/2$, $-2n$, $-2n-1$, where n is a positive integer.

Conclusions

Potential flow models have been explored for jet-flapped supercavitating hydrofoils with finite cavities. The main results are summarized as follows:

1) Among the flow models of a jet-flapped hydrofoil with a finite cavity; open model, semiclosed model and closed model, only the open model is reasonable from a theoretical viewpoint.

2) The integro-differential equations of the jet slope are solved by the method of matched asymptotic expansions in the case of the small-jet momentum flux C_j. Then, the flow regions must be divided to the four regions; near the trailing edge, downstream region, near the termination of the cavity, and far downstream region.

3) The relation between the cavitation number and the cavity length is analyzed and the cavity shape is calculated.

4) Moreover, the lift coefficients are calculated and compared with the experimental results. The present analysis is found to be fairly reasonable.

Appendix

Using $G(s+1)/G(s)=\Gamma(s)$,[11] the following relation is easily proved:

$$Q_0(s+2)=\cot(\pi s)Q_0(s)$$

Moreover, applying the following relation[11]

$$d[\log\psi(s)]/ds=\pi s\cot(\pi s)-\log(2\pi)$$

then

$$Q_0(s)=\left[\frac{\cos^2(\pi s/2)\sin(\pi/4+\pi s/2)}{\cos^3(\pi/4+\pi s/2)}\right]^{1/2}$$

$$\times\exp\left[-\int^s\frac{\pi s}{\sin(\pi s)}ds+\int^s\frac{\pi s}{\cos(\pi s)}ds\right]$$

References

[1] Williams, J., "British Research on the Jet-Flap Scheme," *Zeitschrift fur Flugwissenschaften*, Vol. 6, 1958, pp. 170-176.

[2] Ho, H. T., "The Linearized Theory of a Supercavitating Hydrofoil With a Jet Flap," *ASME Transactions, Journal of Basic Engineering*, Ser. D., Vol. 91, Dec. 1969, pp. 851-860.

[3] Kida, T. and Miyai, Y., "Wall Effect in Cavitating Flow past a Thin Jet-Flapped Foil," *Quarterly Journal of Mechanics and Applied Mathematics*, Vol. 25, 1972, pp. 83-103.

[4] Ho, H. T., "Hydrodynamic Characteristics of a Cambered Hydrofoil With a Jet Flap," *ASME Transactions, Journal of Applied Mechanics*, Ser. E, Vol. 39, June 1972, pp. 337-344.

[5] Oba, R. and Higuchi, G., "Hydrodynamic Characteristics of Supercavitating Jet-Flapped Foils (First Report)," preprint of Japan Society of Mechanical Engineers, No. 720-4, 1972, pp. 157-160 (in Japanese).

[6] Dinh, N. N., "Some Experiments on a Supercavitating Plane Hydrofoil with Jet Flap," *Journal of Ship Research*, Sept. 1969, pp. 207-219.

[7] Spence, D. A., "The Lift Coefficient of a Thin, Jet-Flapped Wing," *Proceedings of the Royal Society (London)*, Ser. A, Vol. 238, 1956, pp. 46-68.

[8] Tulin, M. P., "Supercavitating Flows—Small Perturbation Theory," *Journal of Ship Research*, Jan. 1964, pp. 16-37.

[9] Nishiyama, T. and Ota, T., "Linearized Potential Flow Models for Hydrofoils in Supercavitating Flows," *ASME Transactions, Journal of Basic Engineering*, Ser. D, Vol. 93, Dec. 1971, pp. 550-564.

[10] Kida, T. and Miyai, Y., "A First- and Second-Order Theory on a Supercavitating Hydrofoil with a Jet Flap," *ASME Transactions, Journal of Applied Mechanics*, Ser. E., to be published.

[11] Spence, D. A., "The Lift Coefficient of a Thin Jet-Flapped Wing II: A Solution of the Integro-Differential Equation for the Slope of the Jet," *Proceedings of the Royal Society (London)*, Ser. A, Vol. 261, 1961, pp. 97-118.